





EDITOR'S CHOICE

Neuronatin promotes SERCA uncoupling and its expression is altered in skeletal muscles of high-fat diet-fed mice

Jessica L. Braun^{1,2,3} , Allen C. T. Teng^{4,5}, Mia S. Geromella^{1,2,3}, Chantal R. Ryan^{3,6}, Rachel K. Fenech^{3,6}, Rebecca E. K. MacPherson^{3,6} , Anthony O. Gramolini^{4,5} and Val A. Fajardo^{1,2,3}

- 1 Department of Kinesiology, Brock University, St. Catharines, Canada
- 2 Centre for Bone and Muscle Health, Brock University, St. Catharines, Canada
- 3 Centre for Neuroscience, Brock University, St. Catharines, Canada
- 4 Department of Physiology, University of Toronto, Canada
- 5 Translational Biology and Engineering Program, Ted Rogers Centre for Heart Research, Toronto, Canada
- 6 Department of Health Sciences, Brock University, St. Catharines, Canada

Correspondence

V. A. Fajardo, Department of Kinesiology, Brock University, 1812 Sir Isaac Brock Way, St. Catharines, ON L2S 3A1, Canada E-mail: vfajardo@brocku.ca

(Received 26 June 2021, revised 7 October 2021, accepted 15 October 2021, available online 5 November 2021)

doi:10.1002/1873-3468.14213

Edited by László Nagy

Neuronatin (NNAT) is a transmembrane protein in the endoplasmic reticulum involved in metabolic regulation. It shares sequence homology with sarcolipin (SLN), which negatively regulates the sarco(endo)plasmic reticulum Ca²⁺ATPase (SERCA) that maintains energy homeostasis in muscles. Here, we examined whether NNAT could uncouple the Ca²⁺ transport activity of SERCA from ATP hydrolysis, similarly to SLN. NNAT significantly reduced Ca²⁺ uptake without altering SERCA activity, ultimately lowering the apparent coupling ratio of SERCA. This effect of NNAT was reversed by the adenylyl cyclase activator forskolin. Furthermore, soleus muscles from high fat diet (HFD)-fed mice showed a significant downregulation in NNAT content compared with chow-fed mice, whereas an upregulation in NNAT content was observed in fast-twitch muscles from HFD- versus chow- fed mice. Therefore, NNAT is a SERCA uncoupler in cells and may function in adaptive thermogenesis.

Keywords: calcium transport; forskolin; metabolism; obesity; sarcolipin; sarcoplasmic reticulum

The sarco(endo)plasmic reticulum Ca²⁺-ATPase (SERCA) pump is responsible for maintaining Ca²⁺ homeostasis in innervated cells. Using the energy harnessed from ATP hydrolysis, it catalyzes the transport of Ca²⁺ ions from the cytosol against a concentration gradient (~ 10 000-fold) and into the sarco(endo)plasmic reticulum (SR/ER) in striated muscles [1,2]. SERCA is well-known for its role in

muscle where it regulates muscle relaxation by restoring resting intracellular calcium ([Ca²⁺]_i) and indirectly ensuring sufficient SR Ca²⁺ load for subsequent contractions [3–5]. Furthermore, SERCA plays a significant role in energy homeostasis in muscles, where it accounts for a large proportion (40–50%) of resting energy expenditure, and up to 20% of total daily energy expenditure [6–8].

Abbreviations

BCA, bicinchoninic acid; EDL, extensor digitorum longus; HEK cells, human embryonic kidney cells; HFD, high fat diet; NADH, nicotinamide adenine dinucleotide hydrogen; NNAT, neuronatin; PKA, Protein Kinase A; PLN, phospholamban; RG, red gastrocnemius; RT-qPCR, real-time quantitative PCR; SEM, standard error of the mean; SERCA, sarco(endo)plasmic reticulum Ca²⁺ ATPase; SLN, sarcolipin; SR/ER, sarco(endo)plasmic reticulum; TBP, TATA-box binding protein; TBST, tris-buffered saline tween; UCP-1,uncoupling protein 1; WG, white gastrocnemius; WT, wild-type.

Thus, SERCA has become recognized as a metabolic hub, and altering its energetic contribution in muscle may alter whole body energy homeostasis [8,9]. Based on its structural design and thus binding capacity, SERCA has an optimal coupling ratio of 2 Ca²⁺ ions transported per 1 ATP hydrolyzed [1,2,10–14]; however, lowering the Ca²⁺ transport efficiency of SERCA can increase its energy expenditure, having implications for conditions such as obesity [9,15–17].

There are two well-studied regulators of SERCA phospholamban (PLN) and sarcolipin (SLN) [18-23]. Each interacts and negatively regulates SERCA activity by reducing its affinity for intracellular Ca²⁺ [18– 21]; however, SLN has the unique feature of uncoupling Ca²⁺ transport from ATP hydrolysis [22,23]. Evidently, altering this coupling ratio can change SERCA energy expenditure and thus whole-body energy balance in vivo. For example, Sln-null mice have lowered whole-body energy expenditure and are more susceptible to diet-induced obesity in comparison to wild-type (WT) littermates [15,24]. Conversely, skeletal musclespecific overexpression of SLN in mice results in higher energy expenditure and protects against dietinduced obesity [25]. Given the rising rates of obesity worldwide, impetus has been placed on finding novel ways to increase SLN expression or in the discovery of proteins akin to SLN that also uncouple SERCA in skeletal muscle.

Neuronatin (NNAT) was initially discovered in rat brain tissue where it was shown to regulate the intracellular Ca²⁺ signals necessary for brain development [26–28]. The NNAT gene is alternatively spliced into an 81-amino acid α (canonical) isoform and a 54 amino acid β isoform [29]. We have recently shown the α isoform to be consistently expressed in murine skeletal muscle [30], which is highly conserved across mammalian genomes, with only one different amino acid between human and mouse NNAT (Fig. S1A). In addition to muscle, NNAT has been previously detected in the hypothalamus [31], pancreatic β-cells [32], and adipose tissue [33], suggesting it is involved in appetite regulation, insulin secretion, and adipocyte differentiation, respectively, thereby highlighting its versatile metabolic role [30]. Unlike the topology of PLN and SLN where the C-terminal is in the SR lumen and N-terminal is in the cytosol, NNAT has been predicted [29], and later shown [34], to have "reverse" topology with its N-terminal in the SR and Cterminal in the cytosol. In this orientation, NNAT has shown sequence homology with PLN (ref. [29] and Fig. S1B), and SLN—specifically in its transmembrane domain (Fig. S1C). Based on this sequence homology with both PLN and SLN, NNAT could have a

putative role in regulating the SERCA pump. In support of this, both isoforms possess a single transmembrane domain and have been found localized to the ER in the aforementioned tissues [27,28,35,36]. Furthermore, we have shown NNAT α can bind to both SERCA1a and SERCA2a in murine muscle [30]. Finally, multiple studies have shown that both NNAT isoforms can increase [Ca²⁺]_i in neurons [26–28], adipocytes [36], pancreatic β-cells [35], and human osteosarcoma cells [37]; however, whether NNAT can promote SERCA uncoupling similar to that of SLN has not been investigated. Indeed, like Sln-null mice, Nnat-null mice were previously shown to have lowered whole body energy expenditure and increased susceptibility to high fat diet (HFD)-induced obesity and glucose intolerance compared with WT mice [38]. Furthermore, work investigating epigenetic determinants of obesity found that obesity can be triggered in an "on/ off" manner with the "on" state characterized by reduced Nnat expression [39]. Importantly, the underlying cellular mechanisms behind these findings remain unknown. Thus, in this study, we examined the role of NNAT as a SERCA uncoupler using human embryonic kidney (HEK) cells co-transfected with SERCA1a or SERCA2a and increasing amounts of NNAT. In addition, we measured NNAT protein levels in skeletal muscles of chow- and HFD-fed mice to determine whether NNAT protein expression is altered in response to high-fat feeding.

Materials and Methods

Cell culture and co-transfection of HEK-293 cells

HEK-293 cells were maintained in Dulbecco's modified eagle medium supplemented with 10% FBS, penicillin, and streptomycin. Plasmid DNA encoding for rabbit SER-CA1a, rabbit SERCA2a, and human NNAT (Genescript, Clone ID, OHu21175D, Piscataway, NJ, USA) were used for co-transfection experiments. pBluescript was included as a filler plasmid as indicated in figures. All cells (passages 8-12) were transfected with a total 6 μg of DNA using polyethylenimine reagent as previously described [40]. Cotransfection of SERCA1a or SERCA2a with NNAT was done at 1:1 (1 µg SERCA + 1 µg NNAT + 4 µg of pBluescript DNA) and 1:5 cDNA ratios (1 µg SERCA + 5 µg NNAT). Cells transfected with 1 µg of SERCA1a or SERCA2a DNA and 5 µg of pBluescript served as our controls (SERCA: NNAT, 1:0). All cells were harvested 48 h after transfection in an ice-cold solution of PBS (137 mm NaCl, 10 mm phosphate, 2.7 mm KCl, pH 7.4) containing 5 mm EDTA. The cells were then pelleted by centrifugation at 1500 g for 5 min at 4 °C and washed twice in ice-cold PBS alone. After removal of the supernatants, the cells were resuspended in assay buffer (250 mm Sucrose, 5 mm HEPES, 0.2 mm PMSF, 0.2% NaN₃, pH 7.5) and stored at -80 °C.

Animals

Forty-eight male C57BL/6 mice (16 weeks old, Jackson Laboratories) were housed in an environmentally controlled room (23-24 °C) with a standard 12: 12 h light-dark cycle. Mice were acclimatized to Brock University's animal facility for 1 week prior to experimental interventions. The mice were then randomly divided into a chow diet (2014 Teklad standard chow, 13% kcal from fat; n = 24) or a HFD (D12492 Research Diets, 60% kcal from fat; n = 24) and had access to food and water ad libitum for 12 weeks. Following the 12-week dietary period, mice were anesthetized with sodium pentobarbital (5 mg/100 g body weight, intraperitoneal injection) and the soleus, extensor digitorum longus (EDL), red gastrocnemius (RG), and white gastrocnemius (WG) muscles were dissected, homogenized (250 mm Sucrose, 5 mm HEPES, 0.2 mm PMSF, 0.2% NaN₃, pH 7.5) and stored at -80 °C until further analysis. All animal procedures were approved by the Brock University Animal Care and Utilization Committee (file #19-04-01) and were carried out in accordance with the Canadian Council on Animal Care guidelines.

Western blotting

Western blotting was used to assess NNAT, SERCA2a, and SERCA1a protein content in the HEK cell lysates and skeletal muscle homogenates as previously described [30,41]. A bicinchoninic acid assay was used to determine protein concentration and a total protein load of 15 µg was used for NNAT in HEK cells, soleus, EDL, and RG and 40 µg for the WG. Three micrograms of protein was loaded to detect SERCA2a in HEK cells and soleus and 10 µg was loaded for the EDL, RG, and WG. Finally, 10 µg of protein was loaded to detect SERCA1a in HEK cells and the soleus and 3 µg was loaded for the EDL, RG, and WG. HEK cell lysates and skeletal muscle homogenates were solubilized in Laemmli buffer (#161-0747; BioRad, Hercules, CA, USA), separated by SDS/PAGE with TGX BioRad PreCast 4-15% gradient gels (#4568086; BioRad), and transferred to a polyvinylidene difluoride membrane using the BioRad Transblot Turbo. All membranes were blocked in 5% (w/v) non-fat milk in Trisbuffered saline + 0.1% (V/V) Tween 20 [tris-buffered saline tween (TBST)] for 1 h at room temperature before the addition of primary antibody. The primary antibody for NNAT was obtained from Proteintech (26905-1-AP, Rosemont, IL, USA) and was applied at a 1:1000 dilution in 5% milk overnight at 4 °C. The SERCA1a and SERCA2a antibodies were obtained from ThermoFisher Scientific (Waltham, MA, USA, MA3-911, and MA3-919) and were

applied at a 1:5000 dilution in 5% milk overnight at 4 °C. After washing 3X in TBST, corresponding anti-rabbit (NNAT, 1:10 000) and anti-mouse (SERCA1a and SERCA2a, 1:20 000) antibodies were then applied the next day for 1 h at room temperature in 5% milk. Following another three washes in TBST, the antigen-antibody complexes were captured using Immobilon® enhanced chemiluminescence Ultra Western horseradish peroxidase Substrate (MilliporeSigma, Burlington, MA, USA) and a BioRad ChemiDoc Imager. A Ponceau stain was used to assess total protein loads. All images, including Ponceau stains were quantified using IMAGELAB software (BioRad) and target protein amounts were normalized to total protein detected with a Ponceau stain.

qRT-PCR analyses

Two days following transfection, total RNA extraction from transfected HEK-293 cells was performed with TRIzol (Sigma, T9424, Oakville, ON, Canada) according to manufacturer's instruction. RNA integrity was assessed by measuring 28S and 18S intensity via bleach gels as previously described [42]. Both reverse transcription-mediated cDNA synthesis (ThermoFisher Scientific, 4387406) and real-time quantitative PCR (qRT-PCR) assays (Thermo-Fisher Scientific, 4367659) were performed per manufacturers' instructions and were compliant with the minimum information for publication of quantitative real-time PCR experiments guidelines [43]. qRT-PCR assays were conducted in CFX384 Real-Time PCR system (Bio-Rad). Validated primers are listed below. 5'-AGA AGA CAG TCC TCT CAC ATC TGG G-3' (Rabbit Serca forward primer). 5'-CGA TGA TGC AGA TCA GCA GGA GA-3' (Rabbit Serca reverse primer). 5'-TAT GAC CCC TAT CAC TCC TG-3' [TATA-box binding protein (TBP) forward primer]. 5'-TTC TTC ACT CTT GGC TCC TGT-3' (TBP reverse primer).

Calcium uptake, SERCA activity, and coupling ratio

Rates of Ca²⁺ uptake were measured in the HEK cells using the Indo-1 Ca²⁺ fluorophore as previously described [15,44–46], but fitted onto a 96-well plate. Briefly, resuspended cells were added to reaction buffer (200 mM KCl, 20 mM HEPES, 10 mM NaN₃, 5 μM *N*,*N*,*N'*,*N'*-tetrakis(2-pyridylmethyl)ethylenediamine, 15 mM MgCl₂, pH 7.0) along with Indo-1 (4 μM final concentration; 57180, Sigma-Aldrich). Samples were plated in duplicate and Ca²⁺ uptake was initiated with ATP (10 mM final concentration). A Molecular Devices M2 plate reader was used to kinetically (shaking the wells prior to each read) measure fluorescence of Ca²⁺-bound Indo-1 (405 nm emission) and Ca²⁺-free Indo-1 (485 nm emission) upon excitation at 355 nm at 37 °C. The ratio of Ca²⁺-bound to Ca²⁺-free Indo-1 (405/

485 nm) along with the known dissociation constant of 250 nm was used to calculate $[Ca^{2+}]_{free}$ [46]. The rates of Ca^{2+} uptake were then measured as the instantaneous velocity (tangent analyses) at $[Ca^{2+}]_{free}$ of 1000 or 1500 nm with all rates then normalized to total protein content.

To calculate the coupling ratio we then performed Ca²⁺-dependent SERCA activity assays in the same resuspended HEK cells using the corresponding [Ca²⁺]_{free} of 1000 or 1500 nm. This enzyme-linked spectrophotometric assay indirectly measures ATP hydrolysis through nicotinamide adenine dinucleotide hydrogen disappearance at 37 °C [41,47]. After normalizing the activity rates to total protein content, SERCA coupling ratio was calculated by dividing the rate of Ca²⁺ uptake by the rate of ATP hydrolysis (i.e., SERCA activity) [15,48].

All Ca²⁺ uptake experiments and SERCA activity assays were first performed both in the absence of oxalate and calcium ionophore (A23187; Sigma C7522), respectively, to mimic physiological conditions [15]. Similar conditions were used to investigate the effect of SLN on SERCA's apparent coupling ratio [15]. In addition, Ca²⁺ uptake experiments and SERCA activity assays in SERCA2a transfected cells were performed in the presence of oxalate and calcium ionophore to represent non-limiting conditions. For these experiments, Ca²⁺ uptake and SERCA activity assays were also performed on SERCA2a transfected cells after a 30 min incubation with or without 50 μM forskolin (F6886; Sigma) on ice prior to each assay.

Statistics

All data are presented as means \pm standard error of the mean (SEM). A one-way ANOVA with a Tukey's *post-hoc* test was used to compare NNAT and SERCA isoform content across all SERCA: NNAT co-transfected cells (1:0 vs 1:1 vs 1:5) as well as to assess differences in Ca²⁺ uptake, SERCA activity, and coupling ratio, specifically comparing means against the control co-transfected HEK cells (1:0 SERCA: NNAT). A Student's *t*-test was used for comparisons between SERCA: NNAT 1:1 vs SERCA: NNAT 1:5 and for HFD vs chow experiments. GRAPHPAD PRISM (San Diego, CA, USA) 8 was used to perform all statistical tests, and statistical significance was set at $P \le 0.05$. Any outliers detected with the ROUT method (Q = 2%) on GRAPHPAD PRISM 8 software was removed prior to analyses.

Results and Discussion

NNAT promotes SERCA uncoupling

We previously showed, through co-immunoprecipitation assays, that NNAT interacted with SERCA2a and SERCA1a in mouse soleus muscles [30]. The function of these protein interactions, however, remains completely

unknown. Here, we first examined whether NNAT would promote uncoupling of SERCA2a in HEK-293 cells cotransfected with SERCA2a and NNAT cDNA at increasing NNAT concentrations. As depicted through our Western blot analyses, NNAT was absent in the control (1:0, SERCA2a: NNAT) HEK cells; however, NNAT increased progressively from 1:1 and 1:5 SERCA2: NNAT co-transfected cells (Fig. 1A,B) with no changes in SERCA2a (Fig. 1C). Our Ca²⁺ uptake assays showed significant and drastic reductions in the rate of Ca2+ uptake when NNAT was transfected at a 1:1 and 1:5 ratio with SERCA2a (Fig. 1D,E). In measuring the rates of SERCA ATPase activity, no significant differences were observed between groups (Fig. 1F). In calculating SERCA's apparent coupling ratio (Ca²⁺ uptake/SERCA activity), significant reductions were seen in both the 1:1 and 1:5 SERCA2a: NNAT co-transfected cells compared with the control cells (Fig. 1G). Together, these results suggest that NNAT promotes SERCA2a uncoupling in transfected HEK cells.

We next sought to determine whether NNAT would promote uncoupling of SERCA1a similarly to SER-CA2a in transfected HEK-293 cells. Again, Western blot analyses show an absence of NNAT in the 1:0 SERCA1a: NNAT co-transfected cells with a progressive increase from 1:1 to 1:5 cells (Fig. 2A,B). Interestingly, we also found a significant and progressive increase in SERCA1a protein from 1:0, 1:1, and 1:5 SERCA1a: NNAT co-transfected cells (Fig. 1A,C). As NNAT protein content increased so too did SERCA1a; however, the reasons for this association remain unknown. In contrast, analyses of SERCA1 mRNA levels show that SERCA1 expression was significantly reduced upon NNAT co-transfection (Fig. S2). A similar finding was observed when examining SERCA2 mRNA levels (Fig. S2). There is a disconnect between mRNA and protein levels for both SERCA1a and SERCA2a as presented in Figs 1 and 2, and Fig. S2, though protein and mRNA content are not always proportionate with one another [49]. Potentially offering an explanation for the increased SER-CA1a protein observed along with NNAT transfection (Fig. 2C), a previous study by Gramolini et al. [50] showed that SLN-SERCA2a binding stabilized one another, thereby increasing SERCA protein half-life. In other P-type ATPases such as the Na⁺/K⁺ ATPase, regulatory subunits are known to serve as a chaperones for the catalytic subunits [51,52]. Although speculative, a similar phenomenon between NNAT and SERCA1a may also occur, where NNAT may chaperone and/or stabilize SERCA1a, however this requires further investigation. In any event, we conducted Ca²⁺ uptake and SERCA activity experiments to determine

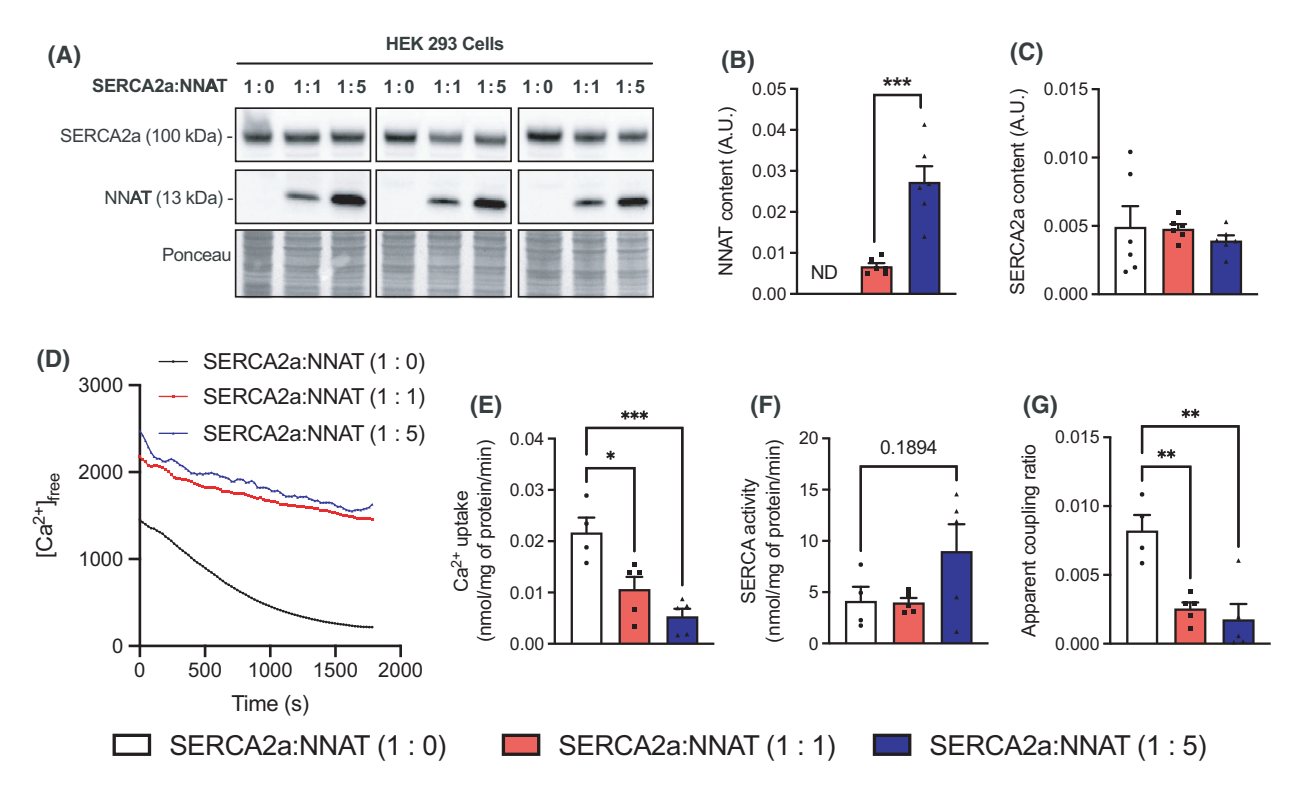


Fig. 1. NNAT promotes uncoupling of SERCA2a in the presence of a Ca^{2+} gradient. (A) Representative Western blot images of NNAT and SERCA2a in HEK co-transfected cells. Ponceau staining was used as a loading control. (B) NNAT and (C) SERCA2a protein content in 1:0, 1:1, and 1:5 SERCA: NNAT co-transfected cells. (D) Change in $[Ca^{2+}]_{free}$ over time after Ca^{2+} uptake was initiated with ATP without oxalate in the buffer in 1:0, 1:1, and 1:5 SERCA: NNAT co-transfected cells. (E) Rates of Ca^{2+} uptake and (F) SERCA ATP hydrolysis (without ionophore) analyzed at a $[Ca^{2+}]_{free}$ of 1500 nm. (G) The calculated apparent coupling ratio (Ca^{2+} uptake/SERCA activity) in 1:0, 1:1, and 1:5 SERCA: NNAT co-transfected cells. Data are means \pm SEM; unpaired Student's t-test (B); one-way ANOVA (C) followed by a Tukey's t-tost (B): t-tost (B

whether NNAT could still show an uncoupling effect. Upon examination of Ca²⁺ uptake, we found that the rates were not significantly different between the 1:0 control cells and the 1:1 SERCA1a: NNAT cells; however, the 1:5 SERCA1a: NNAT cells showed a significant reduction in Ca2+ uptake compared with control cells (Fig. 2D,E). We did not observe any changes in SERCA ATPase activity (Fig. 2F), although the calculated coupling ratio showed trending reductions in the presence of NNAT (Fig. 2G), in both 1:5 and 1:1 SERCA1a: NNAT transfected cells. Thus, despite the complications met with SERCA1 and NNAT transfection, we still observed a significant reduction in Ca²⁺ uptake with no change in SERCA activity leading to trending reductions in SERCA's apparent coupling ratio. This data, though limited, suggest that NNAT inhibits SERCA1a-mediated Ca²⁺ uptake, potentially uncoupling it from ATP hydrolysis.

Our experiments thus far have been performed in the presence of a Ca²⁺ gradient, where the absence of ionophore (SERCA activity) and oxalate (Ca2+ uptake) can lead to back-inhibition of the pump. Though these conditions were also used to showcase the uncoupling effect of SLN under more physiological conditions [15], it is important to determine the effect of NNAT in the absence of a Ca2+ gradient (i.e., nonlimiting conditions with oxalate and ionophore). In this respect, we show that the rate of Ca²⁺ uptake and ATP hydrolysis appears to be faster in SERCA2atransfected HEK-293 cells in the presence of oxalate and ionophore, respectively, which was not entirely surprising (Fig. 3). However, similar to our experiments without oxalate or ionophore (presented in Fig. 1), we find that NNAT significantly reduced Ca²⁺ uptake without altering SERCA activity (Fig. 3A-C). When combined, we again found that NNAT reduced SERCA's apparent coupling ratio even in the absence of a Ca²⁺ gradient. Therefore, our results both in the absence/presence of ionophore and oxalate show that NNAT specifically inhibits SERCA by reducing Ca²⁺

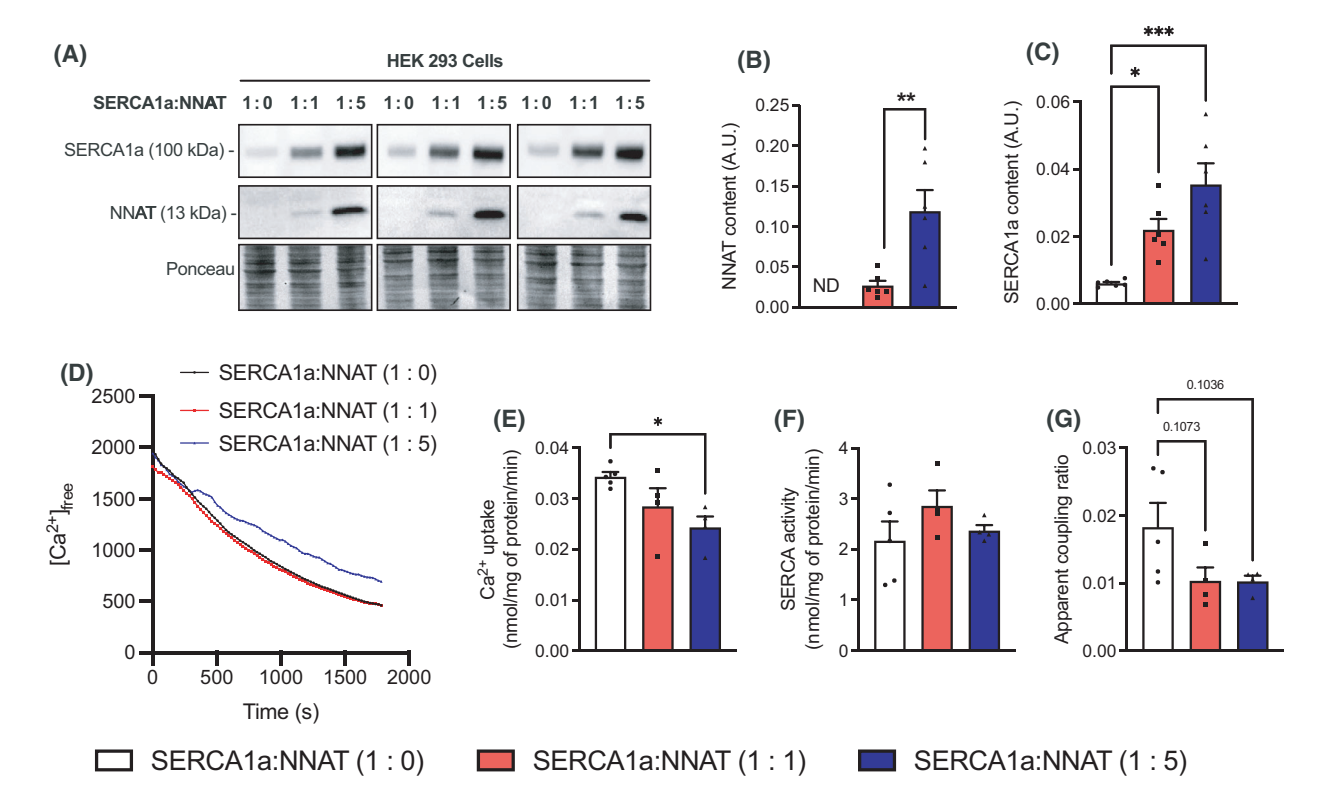
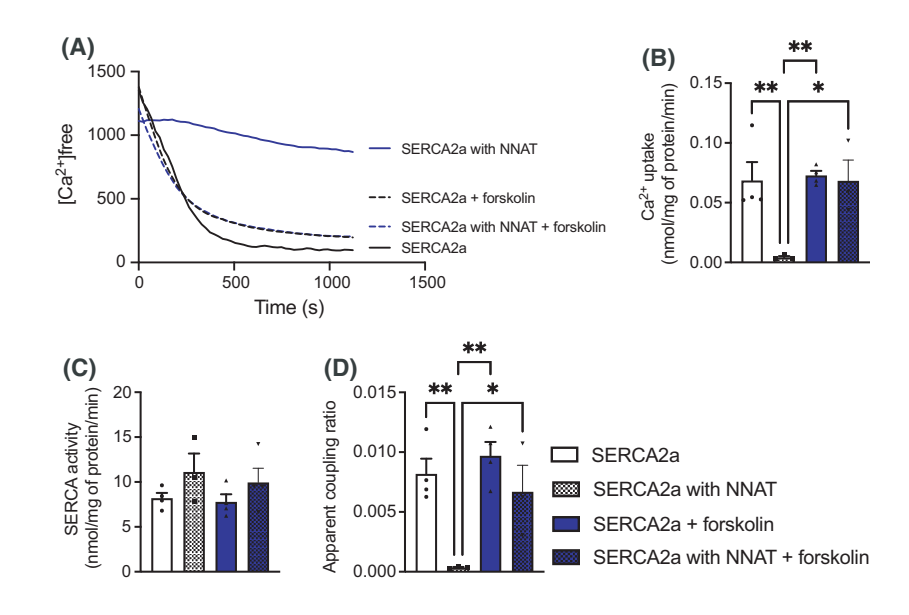


Fig. 2. NNAT reduces SERCA1a-mediated Ca^{2+} uptake. (A) Representative Western blot images of NNAT and SERCA1a in HEK cotransfected cells. Ponceau staining was used as a loading control. (B) NNAT and (C) SERCA2a protein content in 1:0, 1:1, and 1:5 SERCA: NNAT co-transfected cells. (D) Change in $[Ca^{2+}]_{free}$ after the initiation of Ca^{2+} uptake without oxalate in the buffer in the 1:0, 1:1, and 1:5 SERCA: NNAT co-transfected cells. (E) Rates of Ca^{2+} uptake and (F) SERCA ATP hydrolysis (without ionophore) analyzed at a $[Ca^{2+}]_{free}$ of 1500 nm. (G) The calculated apparent coupling ratio $(Ca^{2+}$ uptake/SERCA activity) in 1:0, 1:1, and 1:5 (cDNA) SERCA: NNAT co-transfected cells. Data are means \pm SEM; unpaired Student's \pm -test (B); one-way ANOVA (F) followed by a Tukey's post-hoc (C, E, G). *P < 0.05; **P < 0.01; ***P < 0.005 (n = 4–6 per group, technical replicates from passages 8–12). Values above bars indicate P value.

Fig. 3. NNAT promotes SERCA uncoupling in the absence of a Ca2+ gradient. (A) Change in [Ca²⁺]_{free} over time after Ca2+ uptake was initiated with ATP in 1:5 SERCA: NNAT co-transfected cells in the presence of oxalate and with or without 50 μM forskolin pre-incubation. (B) Rates of Ca²⁺ uptake and (C) SERCA ATP hydrolysis (with ionophore) analyzed at a $[Ca^{2+}]_{free}$ of 1000 nm. (D) The calculated apparent coupling ratio (Ca2+ uptake/ SERCA activity) in HEK cells transfected with SERCA with or without NNAT and with or without forskolin pre-treatment. Data are means ± SEM; one-way ANOVA (C) followed by a Tukey's post-hoc (B, D). *P < 0.05; **P < 0.01 (n = 3-4 per group, technical replicates from passages 8-12).



uptake without altering its ability to hydrolyze ATP. In turn, this mode of inhibition led to the reduction in SERCA's apparent coupling ratio and, in our hands, resembles the Ca²⁺ slippage effect. That is, in the presence of the known uncoupler SLN, Ca²⁺ "slips" off of the SERCA pump after ATP hydrolysis and prior to its transport into the SR/ER [15,23,53], and future studies should investigate whether NNAT regulates SERCA in a similar manner.

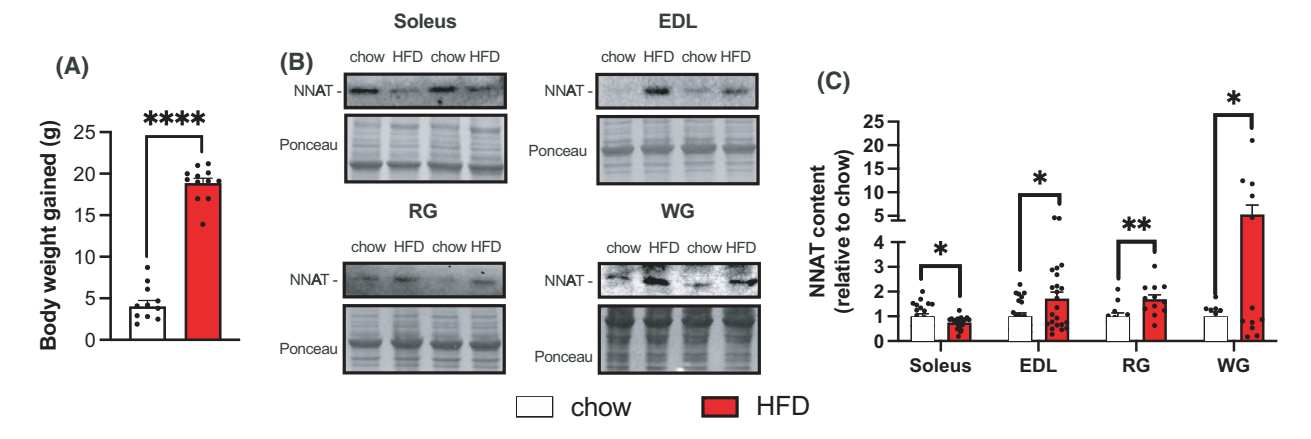
NNAT has a potential phosphorylation site at Ser56 [54], though the physiological role and mechanism of phosphorylation has yet to be investigated. Using kinase-specific phosphorylation prediction software [55], Ser56 phosphorylation is predicted to be mediated through protein kinase A (PKA). As such, we pretreated HEK 293 lysates with 50 µm forskolin prior to conducting the Ca²⁺ uptake and SERCA activity assays. Forskolin is a known adenylyl cyclase activator [56], and strikingly, our results show a complete restoration of Ca²⁺ uptake in SERCA2a: NNAT (1:5) HEK cells (Fig. 3A,B). Furthermore, forskolin had no effect on SERCA activity, which is consistent with our results showing that NNAT does not alter SERCA's ability to hydrolyze ATP. This ultimately restored SERCA's apparent coupling ratio (Fig. 3D). We attribute these findings to a specific effect on NNAT as forskolin treatment in SERCA2a: NNAT 1:0 (cDNA) cells had no effect on Ca²⁺ uptake, SERCA activity or coupling ratio (Fig. 3A-D). Though we suspect this is mediated through NNAT Ser56 phosphorylation, future studies with phosphorvlation-specific NNAT antibodies are required.

It should be noted that our apparent coupling ratio values calculated in this study (with or without NNAT) are far below the expected 2 Ca²⁺ ions transported per ATP hydrolyzed. Though our values are consistent with recently published reports measuring SERCA coupling ratio in the presence and absence of a Ca²⁺ gradient [15,17,48,57], earlier studies have shown coupling ratio values closer to 2 (Ca^{2+} : ATP) [12,13,16,58]. Cornelius and Møller [12] measured the electrogenicity of SERCA-mediated Ca²⁺ transport in reconstituted proteoliposomes and found that ~ 4 electrostatic charges were transferred across the membrane for every ATP hydrolyzed, corresponding to a coupling ratio of 1.8 \pm 0.4 Ca²⁺ per ATP split. Orlowski and Champeil [13] also found that two Ca²⁺ ions were transported into the SR lumen after ATP hydrolysis, and that the dissociation of these two Ca2+ ions from SERCA and into the lumen occurred at a similar rate. Thus, the apparent coupling ratio values presented in this study, and those from recent reports [15,17,48,57] are likely underestimating the true coupling ratio. The

reasons for this discrepancy remain unknown. It has been suggested that the optimal SERCA coupling ratio of 2 can be observed under steady state conditions in the presence of high concentrations of oxalate [58]. However, the addition of oxalate had little effect on the apparent coupling ratio in this study. This was also the case in another recently published study using the same indo-1-based Ca2+ uptake assay and enzymelinked SERCA activity assay [57]. Nevertheless, these two assays and similar experimental conditions were used to showcase the uncoupling effect of SLN [15], albeit again resulting in lower apparent coupling ratio values in muscles obtained from WT and Sln-null mice. Furthermore, in the absence of calculating a coupling ratio, the effect of NNAT on reducing SERCA Ca²⁺ uptake without any effect on SERCA activity provides evidence of uncoupling, as was shown with SLN [53].

NNAT protein content is altered in skeletal muscles of mice fed a HFD

In response to high fat feeding, SLN protein is upregulated 3–5 fold in mouse soleus muscles [22,24] and this is an adaptive response made to combat excessive caloric intake via SLN-mediated SERCA uncoupling. Slnnull mice have reduced whole-body energy expenditure and, when exposed to a HFD, show significantly increased weight gain compared with WT counterparts [15,24]. Similarly, Nnat-null mice present with significant reductions in whole-body energy expenditure and increased weight gain compared with the WT counterparts when fed a HFD [59]; yet the underlying cellular mechanisms remain unknown. Our in vitro experiments showing that NNAT promotes uncoupling of SERCA2a and potentially SERCA1a may offer an explanation. We next sought to determine whether NNAT protein levels would be altered in murine skeletal muscles after high fat feeding. As expected, the HFD group had significantly elevated weight gain compared with the chow-fed mice after 12 weeks of feeding (Fig. 4A). Western blot analyses of NNAT in the soleus, a muscle abundant with NNAT [30], EDL, RG, and WG revealed dynamic and muscle-specific changes in protein content with high fat feeding (Fig. 4B). A significant reduction in NNAT content was observed in the soleus, which contrasted with all other muscles analyzed where NNAT content was significantly increased in the EDL, RG, and, though variable, also in the WG (Fig. 4C). It should be noted that NNAT detection in the WG was relatively difficult as more protein was required to detect NNAT in this muscle (40 µg) compared with the other muscles



analyzed (15 μ g). In addition, these changes in NNAT protein content were, overall, not accompanied with any changes in SERCA2a or SERCA1a protein content (Fig. S3), except for the soleus where a significant reduction in SERCA1a content was observed in the HFD mice compared with the chow-fed mice (Fig. S3B).

The reduction in NNAT protein content in the soleus in response to high fat feeding is opposite of what was previously observed with SLN, which was upregulated 3-5 fold [22,24]. This may represent a physiological advantage, as the presence of both NNAT and SLN in the soleus may cause an overdose of SERCA uncoupling/inhibition compromising muscle health and performance. Conversely, in our hands, we have never detected SLN in the EDL, RG, or WG from WT mice (data not shown). Thus, the increase in NNAT in muscles where SLN is absent, also presents a physiological advantage when responding to HFD, as it could represent a compensatory response aimed at stimulating muscle-based thermogenesis. Indeed, the increased NNAT protein content observed in the EDL, RG, and WG following high fat feeding appear to be in agreement with previous experiments showing that *Nnat*-null mice are more susceptible to an obese phenotype [39] and diet-induced obesity [59]. Taken together, the promotion of SERCA uncoupling in HEK cells and the increases in protein content in muscles that do not express SLN after high-fat feeding suggest that NNAT may work with SLN to regulate muscle-specific energy expenditure via SERCA uncoupling. However, future studies examining the Ser56 phosphorylation status of NNAT could also provide additional insight given our work here showing that forskolin treatment prevents NNAT-mediated SERCA uncoupling.

Future perspectives

In this study, we show for the first time that NNAT promotes SERCA uncoupling by specifically lowering Ca²⁺ uptake without altering ATP hydrolysis, similar to what was found with SLN [53]. This suggests that like SLN, NNAT lowers SERCA Ca²⁺ transport efficiency thereby raising the energetic requirements of the SERCA pump. Typically, two Ca²⁺ ions bind to SERCA in its transmembrane domain, which thereafter allows for the hydrolysis of ATP ultimately powering Ca²⁺ transport into the SR/ER [15,23,60]. However, in the presence of SLN, Ca²⁺ "slips" off of the SERCA pump after ATP hydrolysis and prior to its transport into the SR/ER [15,23]. Whether NNAT uncouples SERCA via a similar slippage mechanism should be investigated further. Moreover, forskolin experiments conducted here suggest that PKA activation can prevent NNAT's ability to uncouple SERCA by restoring Ca²⁺ uptake. Whether this is due to Ser56 phosphorylation of NNAT should be investigated further.

Through its promotion of SERCA uncoupling and muscle-based thermogenesis, SLN has become an attractive target in the fight against obesity. Based on the findings presented here, future studies should also determine whether NNAT may mediate muscle-based thermogenesis via SERCA uncoupling. Importantly, NNAT is more diversely expressed than SLN [30,61]. SLN is expressed solely in muscle, whereas NNAT mRNA and protein can be found in both muscle and

adipocytes [30,61]. Uncoupling protein 1 (UCP-1) is another thermogenic protein found in brown and beige adipocytes where it acts to uncouple mitochondrial respiration from ATP production [62]. In the absence of UCP-1, SERCA-dependent Ca²⁺ cycling has been shown to compensate [63]; however, the exact mechanisms remain undetermined. The role of NNAT as a SERCA uncoupler and its known presence in adipose tissue may provide a potential explanation. Therefore, it is possible that NNAT may be a mediator of both muscle- and adipose-based thermogenesis. Indeed, human studies have also shown that NNAT mRNA is lowered in adipose tissue obtained from obese individuals [33]. In addition to lowered adipose NNAT mRNA, single nucleotide polymorphisms in the NNAT gene have been associated with childhood and adulthood obesity [64]. Thus, it would also be of a great interest to determine whether these mutations alter NNAT regulation of energy metabolism in skeletal muscle and adipocytes via SERCA.

Conclusions

Based on its sequence homology with SLN, we hypothesized and tested whether NNAT would also uncouple SERCA-mediated Ca²⁺ transport from ATP hydrolysis. Using HEK co-transfected cells, we found that NNAT promoted uncoupling of SERCA2a and potentially SERCA1a, though our findings were complicated with unexpected increases in SERCA1a protein occurring with NNAT cDNA transfection. Nonetheless, NNAT uncoupled SERCA2 in the presence and absence of a Ca2+ gradient, and this effect was negated with forskolin pre-treatment, suggestive of a role of PKA and NNAT phosphorylation. In vivo, we found that mice fed a HFD showed muscle-specific changes in NNAT protein content with a significant reduction in NNAT in the soleus, but higher NNAT content in the EDL, RG and WG. Collectively, these findings provide a potential mechanistic explanation as to why Nnat-null mice have lowered whole-body energy expenditure and increased susceptibility to HFD-induced obesity. Future studies should further examine whether NNAT may uncouple SERCA specifically in muscle and adipose tissue. This, in addition to its other roles in metabolism [30] would make NNAT a viable therapeutic target for obesity.

Acknowledgements

The authors thank Wenping Li for excellent technical assistance in these studies. JLB was supported by a Natural Sciences and Engineering Research Council of

Canada (NSERC) undergraduate student research award. RKF was supported by NSERC and an Ontario Graduate Scholarship in Science and Technology (OGS). CRR is supported by OGS. This work was supported by a NSERC Discovery Research grant to VAF (RGPIN 2019-05833) and a Brock Explore Grant to REKM. VAF and AOG were supported by Canada Research Chair (Tier II) awards.

Data accessibility

The data that support the findings of this study are available from the corresponding author [vfa-jardo@brocku.ca] upon reasonable request.

Author contributions

JLB conceptualization, investigation, methodology, formal analysis, data curation, visualization, writing—original draft, writing—review & editing. ACTT investigation, methodology, data curation, writing—review & editing. MSG investigation, methodology, data curation, writing—review & editing. CRR investigation, data curation, writing—review & editing. RKF investigation, data curation, writing—review & editing. REKM funding acquisition, resources, supervision, writing—review & editing. VAF conceptualization, formal analysis, visualization, project administration, funding acquisition, supervision, writing—original draft, writing—review & editing.

References

- 1 Toyoshima C (2007) Ion pumping by calcium ATPase of sarcoplasmic reticulum. In. Ebashi S., Ohtsuki I., Regulatory Mechanisms of Striated Muscle Contraction, pp. 295–303. Tokyo: Springer.
- 2 Toyoshima C, Nakasako M, Nomura H and Ogawa H (2000) Crystal structure of the calcium pump of sarcoplasmic reticulum at 2.6 Å resolution. *Nature* **405**, 647–655.
- 3 Periasamy M and Kalyanasundaram A (2007) SERCA pump isoforms: their role in calcium transport and disease. *Muscle Nerve* **35**, 430–442.
- 4 Periasamy M and Huke S (2001) SERCA pump level is a critical determinant of Ca(2+)homeostasis and cardiac contractility. *J Mol Cell Cardiol* **33**, 1053–1063.
- 5 Misquitta CM, Mack DP and Grover AK (1999) Sarco/ endoplasmic reticulum Ca2+ (SERCA)-pumps: link to heart beats and calcium waves. *Cell Calcium* 25, 277–290.
- 6 Rolfe DF and Brown GC (1997) Cellular energy utilization and molecular origin of standard metabolic rate in mammals. *Physiol Rev* 77, 731–758.

- 7 Fuller-Jackson J-P and Henry BA (2018) Adipose and skeletal muscle thermogenesis: studies from large animals. *J Endocrinol* 237, R99–R115.
- 8 Smith IC, Bombardier E, Vigna C and Tupling AR (2013) ATP consumption by sarcoplasmic reticulum Ca²⁺ pumps accounts for 40-50% of resting metabolic rate in mouse fast and slow twitch skeletal muscle. *PLoS ONE* **8**(7), e68924. https://doi.org/10.1371/journal.pone.0068924
- 9 Gamu D, Juracic ES, Hall KJ and Tupling AR (2020) The sarcoplasmic reticulum and SERCA: a nexus for muscular adaptive thermogenesis. *Appl Physiol Nutr Metab* 45, 1–10.
- 10 Dupont Y (1982) Low-temperature studies of the sarcoplasmic reticulum calcium pump. Mechanisms of calcium binding. *Biochim Biophys Acta* 688, 75–87.
- 11 Clarke DM, Loo TW, Inesi G and MacLennan DH (1989) Location of high affinity Ca2+-binding sites within the predicted transmembrane domain of the sarcoplasmic reticulum Ca2+-ATPase. *Nature* **339**, 476–478.
- 12 Cornelius F and Møller JV (1991) Electrogenic pump current of sarcoplasmic reticulum Ca(2+)-ATPase reconstituted at high lipid/protein ratio. FEBS Lett 284, 46–50.
- 13 Orlowski S and Champeil P (1991) The two calcium ions initially bound to nonphosphorylated sarcoplasmic reticulum Ca(2+)-ATPase can no longer be kinetically distinguished when they dissociate from phosphorylated ATPase toward the lumen. *Biochemistry* 30, 11331–11342.
- 14 Møller JV, Olesen C, Winther AM and Nissen P (2010) The sarcoplasmic Ca2+-ATPase: design of a perfect chemi-osmotic pump. *Q Rev Biophys* 43, 501–566.
- 15 Bombardier E, Smith IC, Vigna C, Fajardo VA and Tupling AR (2013) Ablation of sarcolipin decreases the energy requirements for Ca2+ transport by sarco (endo)plasmic reticulum Ca2+-ATPases in resting skeletal muscle. *FEBS Lett* **587**, 1687–1692.
- 16 de Meis L (2002) Ca2+-ATPases (SERCA): energy transduction and heat production in transport ATPases. J Membr Biol 188, 1–9.
- 17 Verkerke ARP, Ferrara PJ, Lin CT, Johnson JM, Ryan TE, Maschek JA, Eshima H, Paran CW, Laing BT, Siripoksup P *et al.* (2019) Phospholipid methylation regulates muscle metabolic rate through Ca(2+) transport efficiency. *Nat Metab* 1, 876–885.
- 18 Antipenko AY, Spielman AI and Kirchberger MA (1997) Comparison of the effects of phospholamban and jasmone on the calcium pump of cardiac sarcoplasmic reticulum. Evidence for modulation by phospholamban of both Ca2+ affinity and Vmax (Ca) of calcium transport. J Biol Chem 272, 2852–2860.
- 19 MacLennan DH and Kranias EG (2003) Phospholamban: a crucial regulator of cardiac contractility. Nat Rev Mol Cell Biol 4, 566–577.

- 20 Babu GJ, Bhupathy P, Timofeyev V, Petrashevskaya NN, Reiser PJ, Chiamvimonvat N and Periasamy M (2007) Ablation of sarcolipin enhances sarcoplasmic reticulum calcium transport and atrial contractility. *Proc Natl Acad Sci USA* 104, 17867–17872.
- 21 Tupling AR, Bombardier E, Gupta SC, Hussain D, Vigna C, Bloemberg D, Quadrilatero J, Trivieri MG, Babu GJ, Backx PH et al. (2011) Enhanced Ca²⁺ transport and muscle relaxation in skeletal muscle from sarcolipin-null mice. Am J Physiol Cell Physiol 301, C841–C849.
- 22 Bal NC, Maurya SK, Sopariwala DH, Sahoo SK, Gupta SC, Shaikh SA, Pant M, Rowland LA, Bombardier E, Goonasekera SA et al. (2012) Sarcolipin is a newly identified regulator of muscle-based thermogenesis in mammals. Nat Med 18, 1575–1579.
- 23 Mall S, Broadbridge R, Harrison SL, Gore MG, Lee AG and East JM (2006) The presence of sarcolipin results in increased heat production by Ca(2+)-ATPase. *J Biol Chem* **281**, 36597–36602.
- 24 Bombardier E, Smith IC, Gamu D, Fajardo VA, Vigna C, Sayer RA, Gupta SC, Bal NC, Periasamy M and Tupling AR (2013) Sarcolipin trumps β-adrenergic receptor signaling as the favored mechanism for muscle-based diet-induced thermogenesis. *The FASEB Journal* 27, 3871–3878. https://doi.org/10.1096/fj.13-230631
- 25 Maurya SK, Bal NC, Sopariwala DH, Pant M, Rowland LA, Shaikh SA and Periasamy M (2015) Sarcolipin is a key determinant of the basal metabolic rate, and its overexpression enhances energy expenditure and resistance against diet-induced obesity. *J Biol Chem* 290, 10840–10849.
- 26 Joseph R, Dou D and Tsang W (1995) Neuronatin mRNA: alternatively spliced forms of a novel brainspecific mammalian developmental gene. *Brain Res* 690, 92–98.
- 27 Lin HH, Bell E, Uwanogho D, Perfect LW, Noristani H, Bates TJ, Snetkov V, Price J and Sun YM (2010) Neuronatin promotes neural lineage in ESCs via Ca(2+) signaling. *Stem Cells* 28, 1950–1960.
- 28 Oyang EL, Davidson BC, Lee W and Poon MM 2011) Functional characterization of the dendritically localized mRNA neuronatin in hippocampal neurons. *PLoS One* **6**, e24879.
- 29 Dou D and Joseph R (1996) Cloning of human neuronatin gene and its localization to chromosome-20q 11.2-12: the deduced protein is a novel "proteolipid'. *Brain Res* **723**, 8–22.
- 30 Braun JL, Geromella MS, Hamstra SI and Fajardo VA (2020) Neuronatin regulates whole-body metabolism: is thermogenesis involved? *FASEB BioAdv* **2**, 579–586.
- 31 Scott WR, Gelegen C, Chandarana K, Karra E, Yousseif A, Amouyal C, Choudhury AI, Andreelli F, Withers DJ and Batterham RL (2013) Differential premRNA splicing regulates Nnat isoforms in the

- hypothalamus after gastric bypass surgery in mice. *PLoS One* **8**, e59407.
- 32 Niwa H, Harrison LC, DeAizpurua HJ and Cram DS (1997) Identification of pancreatic beta cell-related genes by representational difference analysis. *Endocrinology* **138**, 1419–1426.
- 33 Gburcik V, Cleasby ME and Timmons JA (2013) Loss of neuronatin promotes "browning" of primary mouse adipocytes while reducing Glut1-mediated glucose disposal. Am J Physiol Endocrinol Metab 304, E885–E894.
- 34 Millership SJ, Da Silva Xavier G, Choudhury AI, Bertazzo S, Chabosseau P, Pedroni SM, Irvine EE, Montoya A, Faull P, Taylor WR *et al.* (2018) Neuronatin regulates pancreatic β cell insulin content and secretion. *J Clin Invest* 128, 3369–3381.
- 35 Joe MK, Lee HJ, Suh YH, Han KL, Lim JH, Song J, Seong JK and Jung MH (2008) Crucial roles of neuronatin in insulin secretion and high glucose-induced apoptosis in pancreatic beta-cells. *Cell Signal* **20**, 907–915.
- 36 Suh YH, Kim WH, Moon C, Hong YH, Eun SY, Lim JH, Choi JS, Song J and Jung MH (2005) Ectopic expression of neuronatin potentiates adipogenesis through enhanced phosphorylation of cAMP-response element-binding protein in 3T3-L1 cells. *Biochem Biophys Res Commun* 337, 481–489.
- 37 Saeed H, Sinha S, Mella C, Kuerbitz JS, Cales ML, Steele MA, Stanke J, Damron D, Safadi F and Kuerbitz SJ (2020) Aberrant epigenetic silencing of neuronatin is a frequent event in human osteosarcoma. *Oncotarget* 11, 1876–1893.
- 38 Millership SJ, Tunster SJ, Van de Pette M, Choudhury AI, Irvine EE, Christian M, Fisher AG, John RM, Scott J and Withers DJ (2018) Neuronatin deletion causes postnatal growth restriction and adult obesity in 129S2/Sv mice. *Mol Metab* 18, 97–106.
- 39 Dalgaard K, Landgraf K, Heyne S, Lempradl A, Longinotto J, Gossens K, Ruf M, Orthofer M, Strogantsev R, Selvaraj M et al. (2016) Trim28 haploinsufficiency triggers bi-stable epigenetic obesity. Cell 164, 353–364.
- 40 Hakem Zadeh F, Teng ACT, Kuzmanov U, Chambers PJ, Tupling AR and Gramolini AO (2019) AKAP6 and phospholamban colocalize and interact in HEK-293T cells and primary murine cardiomyocytes. *Physiol Rep* 7, e14144.
- 41 Braun JL, Hamstra SI, Messner HN and Fajardo VA (2019) SERCA2a tyrosine nitration coincides with impairments in maximal SERCA activity in left ventricles from tafazzin-deficient mice. *Physiol Rep* 7, 1–9.
- 42 Aranda PS, LaJoie DM and Jorcyk CL (2012) Bleach gel: a simple agarose gel for analyzing RNA quality. *Electrophoresis* **33**, 366–369.
- 43 Bustin SA, Benes V, Garson JA, Hellemans J, Huggett J, Kubista M, Mueller R, Nolan T, Pfaffl MW, Shipley

- GL *et al.* (2009) The MIQE guidelines: minimum information for publication of quantitative real-time PCR experiments. *Clin Chem* **55**, 611–622.
- 44 Fajardo VA, Bombardier E, McMillan E, Tran K, Wadsworth BJ, Gamu D, Hopf A, Vigna C, Smith IC, Bellissimo C et al. (2015) Phospholamban overexpression in mice causes a centronuclear myopathy-like phenotype. Dis Model Mech 8, 999–1009.
- 45 Fajardo VA, Smith IC, Bombardier E, Chambers PJ, Quadrilatero J and Tupling AR (2016) Diaphragm assessment in mice overexpressing phospholamban in slow-twitch type I muscle fibers. *Brain Behav* 6(6), e00470.
- 46 Tupling R and Green H (2002) Silver ions induce Ca²⁺ release from the SR *in vitro* by acting on the Ca²⁺ release channel and the Ca²⁺ pump. *J Appl Physiol* (1985) **92**, 1603–1610.
- 47 Hamstra SI, Kurgan N, Baranowski RW, Qiu L, Watson CJF, Messner HN, MacPherson REK, MacNeil AJ, Roy BD and Fajardo VA (2020) Lowdose lithium feeding increases the SERCA2a-to-phospholamban ratio, improving SERCA function in murine left ventricles. *Exp Physiol* **105**, 666–675.
- 48 Fajardo VA, Bombardier E, Irvine T, Metherel AH, Stark KD, Duhamel T, Rush JW, Green HJ and Tupling AR (2015) Dietary docosahexaenoic acid supplementation reduces SERCA Ca transport efficiency in rat skeletal muscle. *Chem Phys Lipids* 187, 56–61.
- 49 Liu Y, Beyer A and Aebersold R (2016) On the dependency of cellular protein levels on mRNA abundance. *Cell* 165, 535–550.
- 50 Gramolini AO, Kislinger T, Asahi M, Li W, Emili A and MacLennan DH (2004) Sarcolipin retention in the endoplasmic reticulum depends on its C-terminal RSYQY sequence and its interaction with sarco (endo)plasmic Ca(2+)-ATPases. *Proc Natl Acad Sci USA* 101, 16807–16812.
- 51 Tokhtaeva E, Sachs G and Vagin O (2009) Assembly with the Na, K-ATPase alpha(1) subunit is required for export of beta(1) and beta(2) subunits from the endoplasmic reticulum. *Biochemistry* **48**, 11421–11431.
- 52 Geering K (2008) Functional roles of Na, K-ATPase subunits. *Curr Opin Nephrol Hypertens* **17**, 526–532.
- 53 Smith WS, Broadbridge R, East JM and Lee AG (2002) Sarcolipin uncouples hydrolysis of ATP from accumulation of Ca²⁺ by the Ca²⁺-ATPase of skeletal-muscle sarcoplasmic reticulum. *Biochem J* **361**, 277–286.
- 54 Sacco F, Humphrey SJ, Cox J, Mischnik M, Schulte A, Klabunde T, Schäfer M and Mann M (2016) Glucoseregulated and drug-perturbed phosphoproteome reveals molecular mechanisms controlling insulin secretion. *Nat Commun* 7, 13250.
- 55 Blom N, Sicheritz-Pontén T, Gupta R, Gammeltoft S and Brunak S (2004) Prediction of post-translational

- glycosylation and phosphorylation of proteins from the amino acid sequence. *Proteomics* **4**, 1633–1649.
- 56 Insel PA and Ostrom RS (2003) Forskolin as a tool for examining adenylyl cyclase expression, regulation, and G protein signaling. *Cell Mol Neurobiol* **23**, 305–314.
- 57 Gamu D, Juracic ES, Fajardo VA, Rietze BA, Tran K, Bombardier E and Tupling AR (2019) Phospholamban deficiency does not alter skeletal muscle SERCA pumping efficiency or predispose mice to diet-induced obesity. Am J Physiol Endocrinol Metab 316, E432 e442.
- 58 Inesi G and de Meis L (1989) Regulation of steady state filling in sarcoplasmic reticulum. Roles of back-inhibition, leakage, and slippage of the calcium pump. *J Biol Chem* **264**, 5929–5936.
- 59 Millership SJ, Tunster SJ, Van de Pette M, Choudhury AI, Irvine EE, Christian M, Fisher AG, John RM, Scott J and Withers DJ (2018) Neuronatin deletion causes postnatal growth restriction and adult obesity in 129S2/Sv mice. *Mol Metab* 18, 97–106.
- 60 de Meis L (2001) Uncoupled ATPase activity and heat production by the sarcoplasmic reticulum Ca²⁺-ATPase. Regulation by ADP. *J Biol Chem* **276**, 25078–25087.
- 61 Yang W, Yuan W, Peng X, Wang M, Xiao J, Wu C and Luo L (2019) PPAR gamma/Nnat/NF-kappaB axis involved in promoting effects of adiponectin on preadipocyte differentiation. *Mediators Inflamm* 2019, 5618023.

- 62 Ikeda K and Yamada T (2020) UCP1 dependent and independent thermogenesis in brown and beige adipocytes. *Front Endocrinol (Lausanne)* **11**, 498.
- 63 Ikeda K, Kang Q, Yoneshiro T, Camporez JP, Maki H, Homma M, Shinoda K, Chen Y, Lu X, Maretich P et al. (2017) UCP1-independent signaling involving SERCA2b-mediated calcium cycling regulates beige fat thermogenesis and systemic glucose homeostasis. Nat Med 23, 1454–1465.
- 64 Vrang N, Meyre D, Froguel P, Jelsing J, Tang-Christensen M, Vatin V, Mikkelsen JD, Thirstrup K, Larsen LK, Cullberg KB *et al.* (2010) The imprinted gene neuronatin is regulated by metabolic status and associated with obesity. *Obesity (Silver Spring)* 18, 1289–1296.

Supporting information

Additional supporting information may be found online in the Supporting Information section at the end of the article.

Fig. S1. NNAT is highly conserved across mammalian genomes and shares sequence homology with PLN and SLN.

Fig. S2. SERCA1 and SERCA2 mRNA expression is significantly reduced with NNAT co-transfection.

Fig. S3. SERCA2a and SERCA1a protein content in skeletal muscles of mice fed a chow or HFD.